

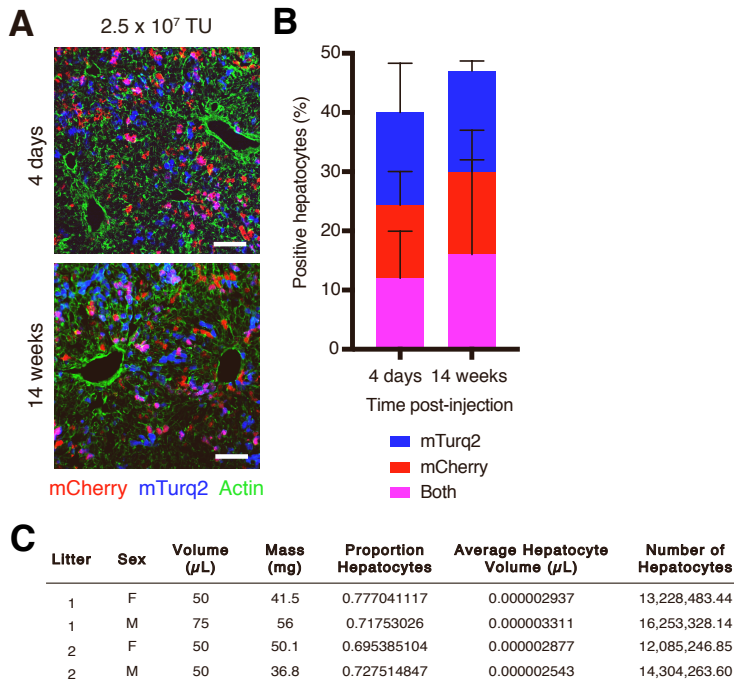
**Cell Genomics, Volume 2**

**Supplemental information**

**Genome-scale CRISPR screening  
in a single mouse liver**

**Heather R. Keys and Kristin A. Knouse**

## Supplemental Figure 1



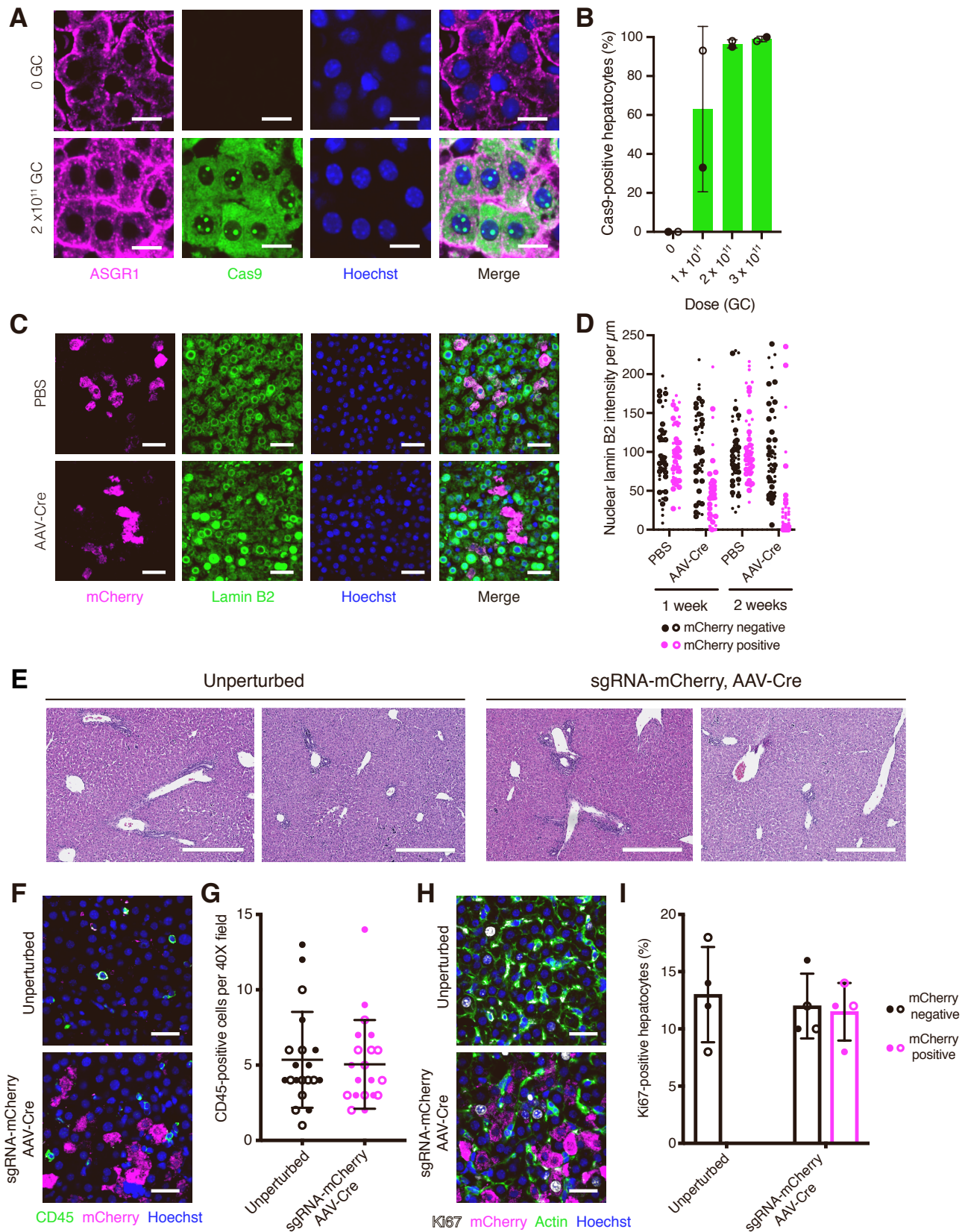
### Supplemental Figure 1. Genome-scale sgRNA delivery in a single mouse liver, Related to Figure 1.

(A) Images of endogenous mCherry and mTurq2 fluorescence in livers from mice four days or 14 weeks after injection of  $2.5 \times 10^7$  TU of an equal mixture of sgAAVS1-mCherry and sgAAVS1-mTurq2 lentiviruses. Scale bars, 100 μm.

(B) Percent mCherry-, mTurq2-, and double-positive hepatocytes in livers from mice four days or 14 weeks after injection of  $2.5 \times 10^7$  TU of an equal mixture of sgAAVS1-mCherry and sgAAVS1-mTurq2 lentiviruses. Error bars indicate standard deviation.  $n = 3$  mice per time point and 200 hepatocytes per mouse.

(C) Table of values used to estimate the number of hepatocytes in postnatal day one livers. Liver volume was measured by volume displacement and percent hepatocytes and hepatocyte volume were measured by immunostaining and microscopy.

## Supplemental Figure 2



## Supplemental Figure 2. Temporally-controlled protein depletion in the mouse liver, Related to Figure 2.

(A) Images of livers from LSL-Cas9 mice injected with 0 or  $2 \times 10^{11}$  GC of AAV-Cre on postnatal day five and harvested four days thereafter immunostained for ASGR1 (hepatocyte marker, magenta) and Cas9 (green) and counterstained with Hoechst (blue). Scale bars, 15  $\mu\text{m}$ .

(B) Percent Cas9-positive hepatocytes in livers from LSL-Cas9 mice injected with varying doses of AAV-Cre on postnatal day five and harvested four days thereafter as determined by Cas9 immunostaining. Bar and whiskers indicate mean and standard deviation across mice, respectively, and closed and open circles represent values from male and female mice, respectively.  $n = 1$  male and 1 female mouse per dose and 200 hepatocytes per mouse.

(C) Images of livers from LSL-Cas9 mice injected with sgLmnb2-mCherry followed by PBS or AAV-Cre immunostained for mCherry (magenta) and lamin B2 (green) and counterstained with Hoechst (blue). Scale bars, 45  $\mu\text{m}$ .

(D) Nuclear lamin B2 intensity per  $\mu\text{m}$  in mCherry-positive and mCherry-negative hepatocytes from LSL-Cas9 mice injected with sgLmnb2-mCherry followed by PBS or AAV-Cre. Closed and open circles represent values from male and female mouse, respectively.  $n = 1$  male and 1 female mouse per condition and 25 cells per mouse.

(E) Images of livers from unperturbed postnatal day 12 LSL-Cas9 mice or postnatal day 12 LSL-Cas9 mice injected with  $1.25 \times 10^7$  TU of sgMaob-mCherry or sgLmnb2-mCherry lentivirus on postnatal day 1 followed by AAV-Cre on postnatal day 5 stained with hematoxylin and eosin. Left and right images represent one male and one female mouse, respectively, from each condition. Scale bars, 300  $\mu\text{m}$ .

(F) Images of livers from unperturbed postnatal day 12 LSL-Cas9 mice or postnatal day 12 LSL-Cas9 mice injected with  $1.25 \times 10^7$  TU of sgMaob-mCherry or sgLmnb2-mCherry lentivirus on postnatal day 1 followed by AAV-Cre on postnatal day 5 immunostained for CD45 (green) and mCherry (magenta) and counterstained for Hoechst (blue). Scale bars, 45  $\mu\text{m}$ .

(G) Number of CD45-positive cells per 40X field in unperturbed postnatal day 12 LSL-Cas9 mice or postnatal day 12 LSL-Cas9 mice injected with  $1.25 \times 10^7$  TU of sgMaob-mCherry or sgLmnb2-mCherry lentivirus on postnatal day 1 followed by AAV-Cre on postnatal day 5 as determined by CD45 immunostaining. Bar and whiskers indicate mean and standard deviation across mice, respectively, and closed and open circles represent values from male and female mice, respectively.  $n = 2$  male and 2 female mice per condition and five fields per mouse.

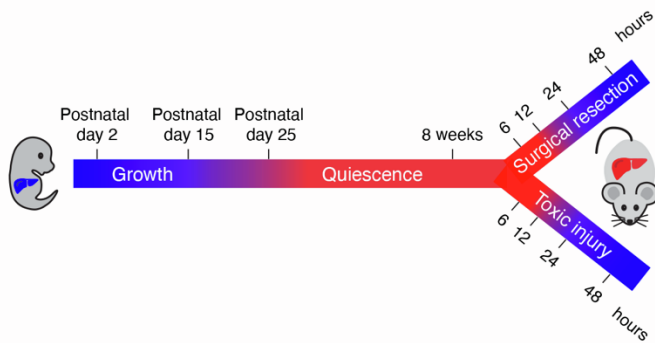
(H) Images of livers from unperturbed postnatal day 12 LSL-Cas9 mice or postnatal day 12 LSL-Cas9 mice injected with  $1.25 \times 10^7$  TU of sgMaob-mCherry or sgLmnb2-mCherry lentivirus on postnatal day 1 followed by AAV-Cre on postnatal day 5 immunostained for Ki67 (white), mCherry (magenta) and actin (green) and counterstained for Hoechst (blue). Scale bars, 45  $\mu\text{m}$ .

(I) Percent Ki67-positive hepatocytes in livers from unperturbed postnatal day 12 LSL-Cas9 mice or postnatal day 12 LSL-Cas9 mice injected with  $1.25 \times 10^7$  TU of sgMaob-mCherry or sgLmnb2-mCherry lentivirus on postnatal day 1 followed by AAV-Cre on postnatal day 5 as determined by Ki67 immunostaining. Bar and whiskers indicate mean and standard deviation across mice, respectively, and closed and open circles represent values from male and female mice, respectively.  $n = 2$  male and 2 female mice per condition and 50 cells per mouse.

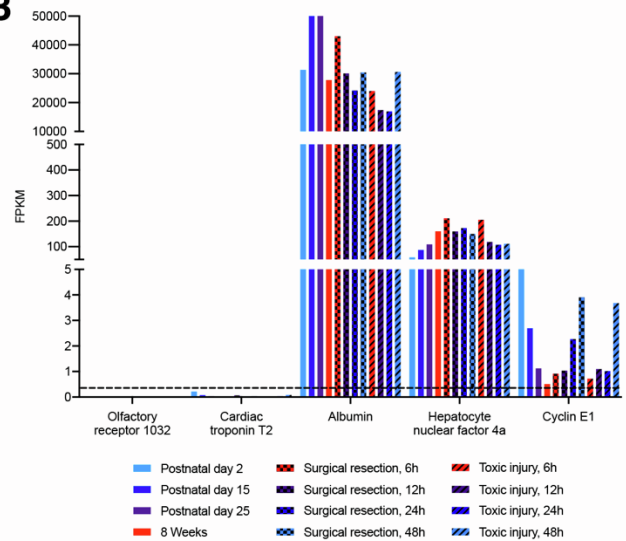


## Supplemental Figure 3

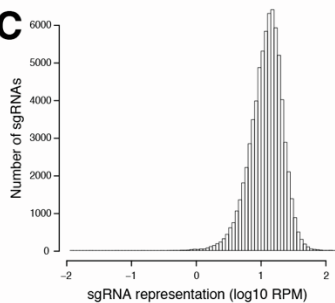
**A**



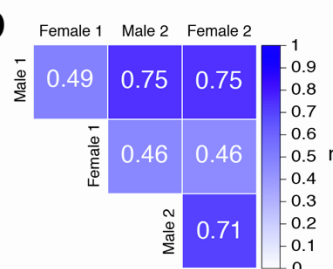
**B**



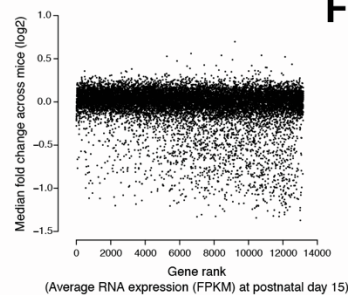
**C**



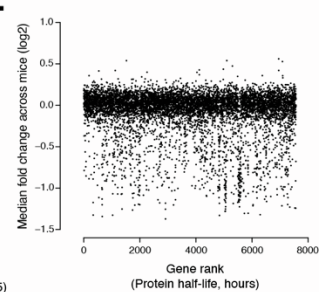
**D**



**E**



**F**



### Supplemental Figure 3. A genome-scale screen for hepatocyte fitness in the neonatal mouse liver, Related to Figure 3.

(A) Time points during liver growth, quiescence, and regeneration from which livers were harvested for RNA sequencing. Partial hepatectomy and carbon tetrachloride were used as surgical resection and toxic injury models, respectively.

(B) Average RNA expression (FPKM) of representative protein-coding genes at different time points of liver growth, quiescence, and regeneration. Dashed line indicates FPKM cutoff of 0.3.  $n = 3$  male mice per time point.

(C) Number of sgRNAs with a given representation ( $\log_{10}$  RPM) for all sgRNAs in the library.

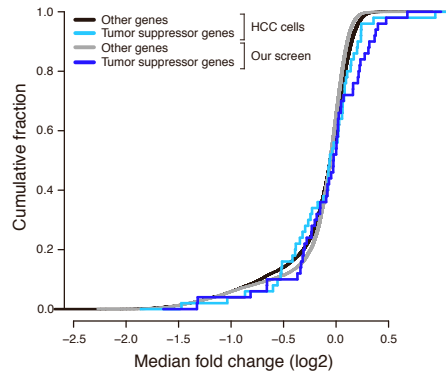
(D) Pearson correlation ( $r$ ) for each plot in Figure 3D.

(E) Median fold change across mice ( $\log_2$ ) of genes ranked by average RNA expression (FPKM) at postnatal day 15 for each gene. Two-sided Spearman  $\rho = -0.15$ ,  $p < 2.2 \times 10^{-16}$ .

(F) Median fold change across mice ( $\log_2$ ) of genes ranked by protein half-life (hours) for each gene. Two-sided Spearman  $\rho = -0.05$ ,  $p = 0.003$ .

## Supplemental Figure 4

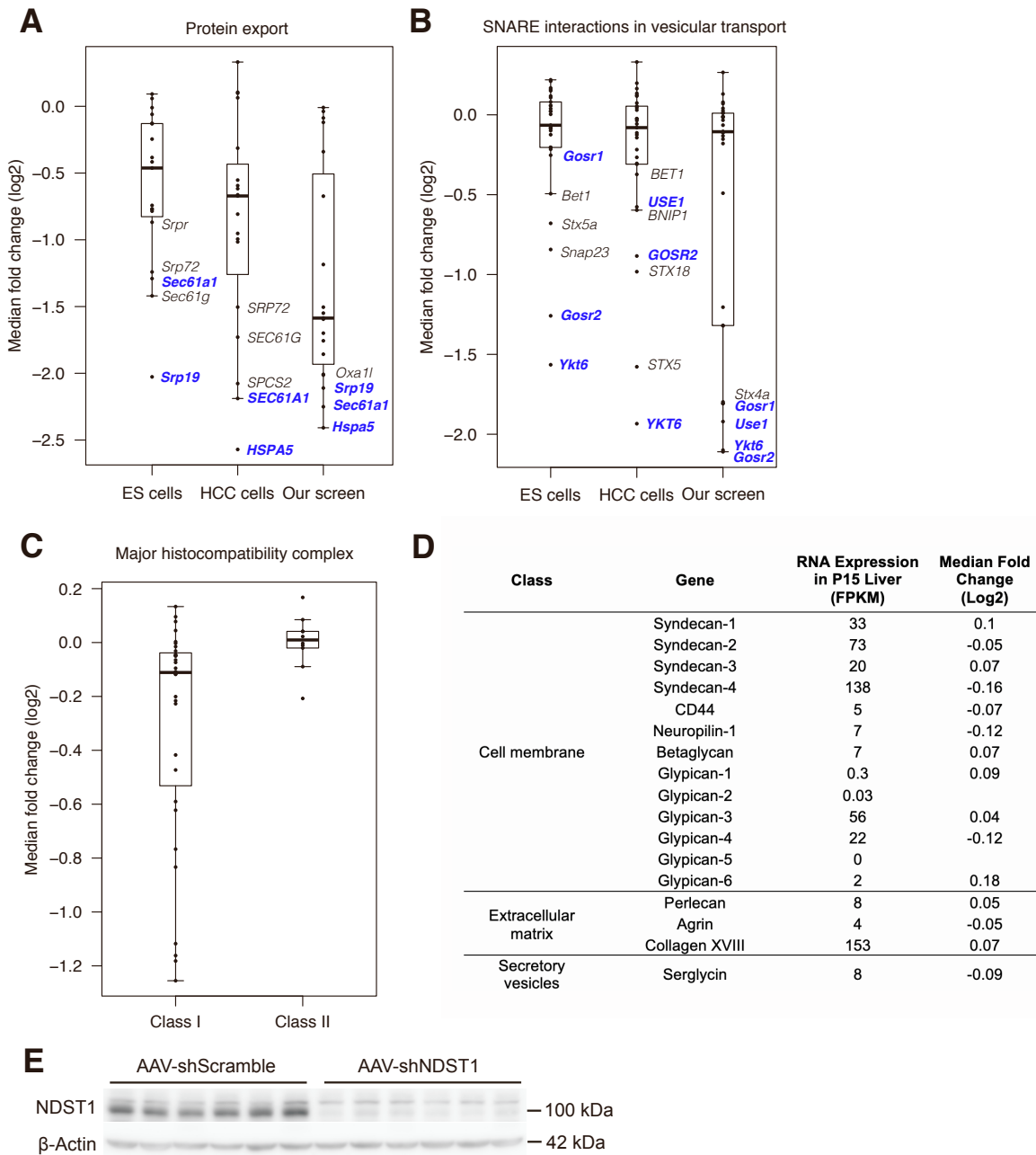
A



### Supplemental Figure 4. Genome-scale screening in the organism enhances discovery of tumor suppressor genes and uncovers genes with sex-specific effects, Related to Figure 4.

(A) Cumulative fraction of tumor suppressor genes (cyan, blue) and other genes (black, grey) based on quantile-normalized median fold change ( $\log_2$ ) of their gene scores across screens in human hepatocellular carcinoma (HCC) cell lines and our screen. HCC cells  $p > 0.05$  by one-sided Kolmogorov-Smirnov test, our screen  $p = 0.0028$  by one-sided Kolmogorov-Smirnov test.

## Supplemental Figure 5



**Supplemental Figure 5. Class I MHC and heparan sulfate biosynthesis are uniquely required for hepatocyte fitness in the organism, Related to Figure 5.** (A) Median fold change (log<sub>2</sub>) of genes in the KEGG gene set for protein export in quantile-normalized ES cell screens, HCC cell line screens, and our screen. Genes depleted in our screen and at least one of the cell culture screens are highlighted in blue. The bounds of the box indicate the first and third quartiles, and the whiskers extend to the furthest data point that is within 1.5 times the interquartile range.

(B) Median fold change (log<sub>2</sub>) for genes in the KEGG gene set for SNARE interactions in vesicular transport in quantile-normalized ES cell screens, HCC cell line screens, and our screen. Genes depleted in our screen and at least one of the cell culture screens are highlighted in blue. The bounds of the box indicate the first and third quartiles, and the whiskers extend to the furthest data point that is within 1.5 times the interquartile range.

(C) Median fold change (log<sub>2</sub>) across mice for genes associated with class I MHC or class II MHC within the KEGG gene set for antigen processing and presentation in our screen. The bounds of the box indicate the first and third quartiles, and the whiskers extend to the furthest data point that is within 1.5 times the interquartile range.

(D) The RNA expression (FPKM) in postnatal day 15 liver and median fold change (log<sub>2</sub>) across mice in our screen for each gene in the three classes of heparan sulfate proteoglycans.

(E) Western blot showing NDST1 protein levels in postnatal day 15 livers injected with  $4 \times 10^{11}$  GC of either AAV-shScramble or AAV-shNDST1 on postnatal day 5. Beta-actin is shown as a loading control. The first three lanes for each condition represent livers from male mice while the last three lanes for each condition represent livers from female mice.